



The transverse and longitudinal beam characteristics of the phin photo-injector at Cern

O. Mete, E. Chevallay, A. Dabrowski, S. Doebert, K. Elsener, V. Fedosseev, T. Lefèvre, M. Petrarca, D. Egger, R. Roux

► To cite this version:

O. Mete, E. Chevallay, A. Dabrowski, S. Doebert, K. Elsener, et al.. The transverse and longitudinal beam characteristics of the phin photo-injector at Cern. 9th European Workshop on Beam Diagnostics and Instrumentation for Particle Accelerators (DIPAC 2009), May 2009, Basel, Switzerland. pp.104-106. in2p3-00477548

HAL Id: in2p3-00477548

<https://hal.in2p3.fr/in2p3-00477548>

Submitted on 29 Apr 2010

HAL is a multi-disciplinary open access archive for the deposit and dissemination of scientific research documents, whether they are published or not. The documents may come from teaching and research institutions in France or abroad, or from public or private research centers.

L'archive ouverte pluridisciplinaire **HAL**, est destinée au dépôt et à la diffusion de documents scientifiques de niveau recherche, publiés ou non, émanant des établissements d'enseignement et de recherche français ou étrangers, des laboratoires publics ou privés.

THE TRANSVERSE AND LONGITUDINAL BEAM CHARACTERISTICS OF THE PHIN PHOTO-INJECTOR AT CERN

O. Mete, CERN, Geneva and EPFL, Lausanne, Switzerland

E. Chevallay, A. Dabrowski, S. Doebert, K. Elsener, V. Fedosseev, T. Lefèvre, M. Petrarca,
CERN, Geneva, Switzerland

D. Egger, EPFL, Lausanne, Switzerland; R. Roux, LAL, Orsay, France

Abstract

The laser driven RF photo-injectors are recent candidates for high-brightness, low-emittance electron sources. One of the main beam dynamics issues for a high brightness electron source is the optimization of beam envelope behavior in the presence of the space charge force in order to get low emittance. Within the framework of the second Joint Research Activity PHIN of the European CARE program, a new photo-injector for CTF3 has been designed and installed by collaboration between LAL, CCLRC and CERN. Beam based measurements have been made during the commissioning runs of the PHIN 2008 and 2009 including measurements of the emittance, using multi-slit technique. The demonstration of the high charge and the stability along the long pulse train are between the goals of this photo-injector study as also being important issues for CTF3 and the CLIC drive beam. In this work the photo-injector will be described and the first beam measurement results will be presented and compared with the PARMELA simulations.

INTRODUCTION

A photo-injector was proposed as a new electron source for CTF3 (CLIC Test Facility 3) and later for the CLIC (Compact Linear Collider) drive beam [1, 2]. After the installation of the PHIN photo-injector at CERN, the longitudinal and the transverse properties of the commissioning beam have been measured in a range of parameters. In laser-driven RF photo-injectors the transverse phase space dynamics are influenced by several issues like time dependency of the RF field, space charge effects and transverse focusing. The adjustment of the laser properties such as spot size, radial and temporal distribution can effectively be used to control the properties of the beam in both directions. During the high charge operation at low energies, the space charge force is the dominating effect for emittance growth. The space charge effect can be compensated with the field created by a focusing magnet. The laser spot size dependence of the transverse size and emittance of the beam has been investigated for the laser spot sizes of 2 mm, 3 mm and 4 mm. The transverse emittance was measured with the multi-slit method in a range of focusing magnet current to study the emittance compensation. This method is applicable to the low energy, space charge dominated beams [3, 4].

01 Overview and Commissioning

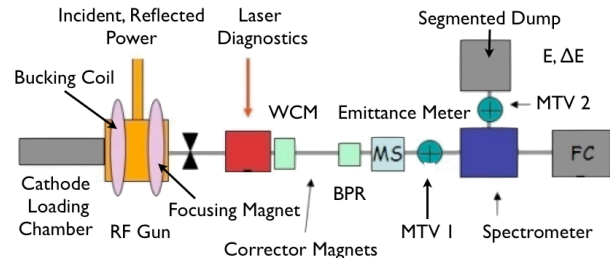


Figure 1: The PHIN photo-injector layout.

SET-UP

The beamline consists of three sections, cathode transfer chamber, RF gun and the beam measurements section (see Fig. 1). A semiconductor $C_{52}Te$ cathode was introduced on one end of a $2+1/2$ cell RF gun in order to extract the electrons. The cathode has been studied at the CERN photo-emission laboratory and demonstrated a lifetime to allow $>100h$ run at a 3% quantum efficiency for a 262 nm laser wavelength. The so called “bucking coil” was installed in parallel to the cathode surface to maintain zero magnetic field in this location. This is to prevent the back-bombardment of the electrons onto the cathode surface that decreases the cathode lifetime and the achievable amount of extracted charge. Another magnet follows in the exit of the gun as a transverse focusing element and ensures the emittance compensation. A Nd:YFL oscillator produces the laser pulses at a repetition rate of 1.5 GHz with an average power of ~ 300 mW. The oscillator has the fundamental wavelength of $\lambda \sim 1047$ nm and a pulse width of $\tau \sim 8$ ps [5]. The laser diagnostics was placed close to the gun as shown in Fig. 1 providing the alignment of the laser and the cathode after the laser table. The third section of the beamline consists of several diagnostics tools: a wall current monitor (WCM) and a beam position RF monitor (BPR) have been included. A set of corrector magnets have been also installed for horizontal and vertical corrections in addition to the focusing magnet. For the emittance measurement a 2 mm thick tungsten multi-slit mask was utilized. The mask has 25 slits each having a width of $100 \mu m$. FLUKA [6] simulations showed that the mask is able to totally stop a 5.5 MeV electron beam allowing the electron transmission only through the windows while 20% of the incoming electrons are backscattered. An OTR (Optical Transition Radiation) screen was used in the system to image the

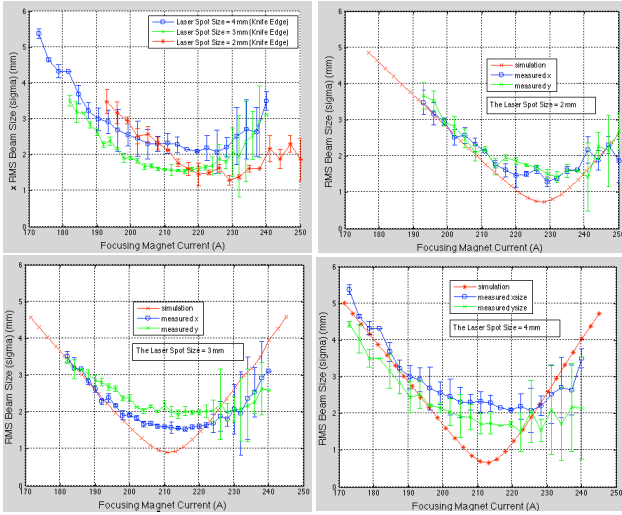


Figure 2: Focusing magnet scans for the transverse beam size measurement for different laser spot sizes.

beamlets after the slits. A Faraday cup was placed after the emittance-meter for charge measurements. The energy spread measurement has been done with a spectrometer, installed in the end of the beamline. The spectrometer consists of a dipole magnet placed before the Faraday cup, a ceramic screen and a CCD camera. When the dipole is active the beam is transmitted to the spectrometer line instead of dumping in the Faraday cup. In the second PHIN run (March 2009), the CCD camera in the emittance-meter has been replaced by a intensified CCD camera allowing to use an aluminum OTR screen. It has been chosen as a better solution than using a more sensitive ceramic screen that often saturates in the usual operation electron intensity. A segmented dump has been also installed and tested in the second PHIN run allowing the measurement of the time resolved longitudinal beam properties.

MEASUREMENTS

For the beam size measurements, simulations depend on the assumption of a round electron beam with a gaussian distribution since the initial properties of the beam resembles the laser properties. As the result of the first run we have observed an asymmetric behavior between the vertical and horizontal components of the beam size. Investigations on the laser alignment and positioning on the cathode, and the background field by the magnetic components in the set-up have been considered as possible sources for this asymmetry. During 2009 run beam size scans have been performed with respect to different laser spot sizes of 2, 3, and 4 mm at 5.5, 5.2 and 5.7 MeV, respectively. The asymmetry was no longer present. The results for that scans are shown in Fig. 2 in comparison with the PARMELA[7] simulations. The simulations and the measurements agree rather well with the exception of the focus region. Al-

01 Overview and Commissioning

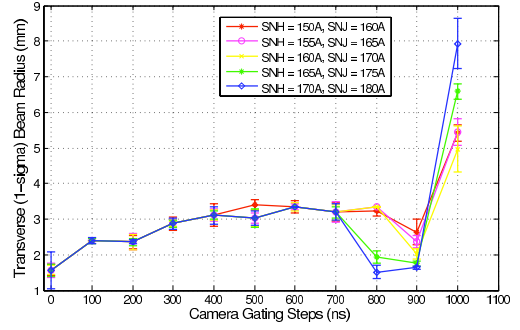


Figure 3: The transverse beam size measurement along the 1.2 μ s long train.

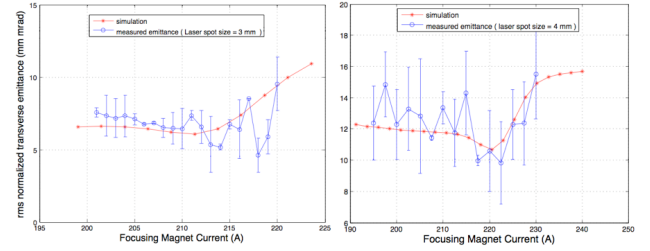


Figure 4: The transverse normalized rms emittance vs focusing magnet current for laser size of 3 mm (left) and 4 mm (right).

though the discrepancy is still under investigation, it could be related to the limited resolution of the optical system or a saturation effect. The transverse emittance and the minimum spot size are scaling with the laser spot size as expected. Since the stability of the beam parameters along a long pulse train is very important for CTF3, the beam size has been measured as a function of time along the train by using a gated camera. The measurement was done with the steps of 100 ns. The gentle increase of the spot size could be explained with an imperfect beam loading compensation during the measurement. The result can be seen on Fig. 3 for different magnet settings. Emittance measurements have been performed over wide a range of focusing magnet current and laser spot size. The emittance scan at energy of 5.7 MeV and 5.2 MeV for the laser spot sizes of 3 mm and 4 mm can be seen in Fig. 4 and compared with the PARMELA simulation. It has been shown that the transverse emittance scales with the laser spot size with the values of around 7 mm mrad at 3 mm and 12 mm mrad for 4 mm laser spot sizes at the focusing region.

The reconstructed phase space can be compared to the PARMELA simulations in Fig. 5. This phase space has been measured as the laser spot size was 3 mm and with the 1.28 nC charge per bunch at 5.2 MeV. The RMS normalized transverse emittance has been measured as 7.3 mm mrad for this given single shot measurement. Time resolved energy of the beam was measured by using a segmented dump. The energy spread was not reliably measurable since a fixed screen in front of the dump caused electron scattering which lead to a factor of 9 widening in the

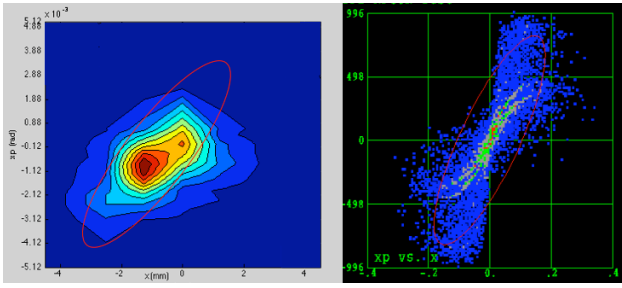


Figure 5: The reconstructed phase space from the measurement (left) and the PARMELA simulation (right).

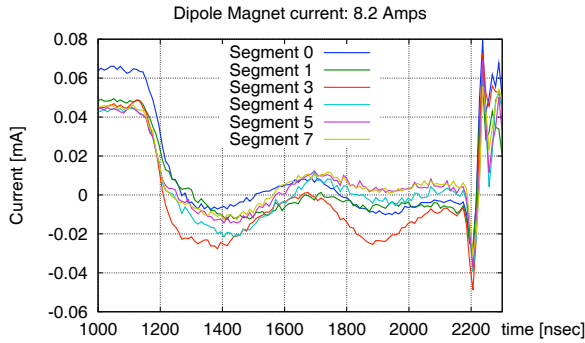


Figure 6: The intensity distribution in the centre of the segmented dump.

transverse size. The screen will be changed to a thin aluminum foil for the next run to avoid this effect. Simulations with GEANT4 [8] showed that the value of energy spread is up to a few percent. Regarding the time resolved aspect of the measurement, the goal was to measure the time variation of the energy along the pulse train. Figure 6 shows the current in the dump for each segment as a function of time. The measurement shows that the energy along the train is stable confirming the stability of the RF system. The beam loading compensation was also studied and optimized by adjusting the timing of the beam versus the RF pulse. Figure 7 shows the successful beam loading compensation. In the presence of the beam, a flat top RF pulse has been obtained resulting in a mono energetic beam. The reflected power is well matched at this point confirming that the in-

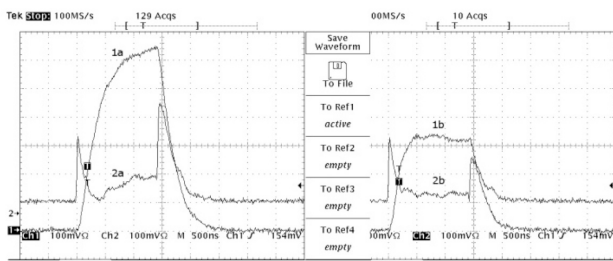


Figure 7: Beam loading. Left: RF power in the gun (1a) and reflected power (2a) when no beam is present. Right: RF power in the gun (1b) and reflected power (2b) when beam is present.

put coupler has been adjusted to the correct over-coupling. The beam was consisted of 300 bunches with a charge of 1.28 nC during the measurements with a laser spot sizes of 3 and 4 mm. The measurements, at 2 mm laser spot size, have been done with a charge of 1.09 nC per bunch. The highest achievable charge was 2.53 nC per bunch during the operation.

CONCLUSION

The beam measurements revealed the expected behavior agreeing with the simulations within some error ranges. The envelope behavior at the small beam sizes has to be investigated considering the possible limitations from the instrumentation and the laser spot size. The emittance measurements have been improved with respect to the previous run by replacing the CCD camera with an intensified one enabling the usage of an aluminum OTR screen. The simulations for the beam size measurements are consistent with the measurements within a 10% error band of the laser spot size. For the segmented dump, simulations showed that elements in the beamline such as the alumina screen significantly increases the transverse size of the beam, due to multiple scattering and energy loss, to the point this contribution is much larger than the dispersion due to energy spread. Although a reliable energy spread measurement was impossible under this condition, the issue will be solved easily in the next commissioning run by replacing the alumina screen with a thin aluminium OTR screen.

REFERENCES

- [1] S. Döbert, "Integration of the PHIN RF Gun into the CLIC Test Facility", MOPLS129, European Particle Accelerator Conference 2006, EPAC'06, Edinburgh, Scotland.
- [2] R. Losito, et. al., "The PHIN Photoinjector for the CTF3 Drive Beam", WEPLS059, European Particle Accelerator Conference 2006, EPAC'06, Edinburgh, Scotland.
- [3] Min Zhang, "Emittance Formula for Slits and Pepper Pot Measurement", FERMILAB-TM-1988.
- [4] S.G. Anderson, "Space-charge Effects in High Brightness Electron Beam Emittance Measurements", Phys. Rev. ST Accel. Beams, APS May, 2002, doi:10.1103/PhysRevSTAB.5.014201.
- [5] M. Petrarca, et al., "First Results From the Commissioning of the PHIN Photo-Injector for CTF3", M06RFP063, Particle Accelerators Conference 2009, PAC'09, Vancouver, Canada.
- [6] A. Ferrari, P.R. Sala, A. Fasso, J. Ranft, "FLUKA: A multi-particle transport code" (Program version 2005), CERN-2005-010.
- [7] L.M. Young, J. Billen, "The Particle Tracking Code PARMELA", Particle Accelerator Conference 2003, PAC'03, Portland, Oregon, USA.
- [8] S. Agostinelli, et.al., "GEANT4: A simulation toolkit", Nucl. Instrum. Meth., A506, 2003, p.250-303, doi:10.1016/S0168-9002(03)01368-8.